Springer

Journal of
Mechanical
Science and
Technology

Journal of Mechanical Science and Technology 22 (2008) 731~739

www.springerlink.com/content/1738-494x

A monolithic silicon multi-sensor for measuring three-axis acceleration, pressure and temperature

Xu Jingbo*, Zhao Yulong, Jiang Zhuangde and Sun Jian

State Key Laboratory of Mechanical Manufacturing System, Xi'an 710049, China

(Manuscript Received May 22, 2007; Revised January 3, 2008; Accepted January 8, 2008)

Abstract

A monolithic multi-sensor for small unmanned aerial vehicles is presented in the paper; it consists of a three-axis piezoresistive accelerometer, a piezoresistive absolute pressure sensor and a silicon thermistor temperature sensor. The accelerometer is designed with four silicon beams supporting the seismic mass and appropriate piezoresistors arrangement to detect three-axis acceleration and greatly reduce cross-axis sensitivities. For minimizing the effect of stress on the temperature sensor, the thermistor is designed along [100] and [010] crystal orientation. The multi-sensor is fabricated on SOI wafers by using MEMS bulk-micromachining technology. Some effective micromachining steps are applied in the fabrication. The two-step wet anisotropic etching process on the backside of the wafers can form the whole backside shape of the multi-sensor. The metal electrode sputtered on the Pyrex glass can avoid sticking between the Pyrex glass and the seismic mass in the process of anodic bonding. The die size of the multi-sensor is $4\times6\times0.9mm^3$. The measured results show that the multi-sensor is appropriate for its application field.

Keywords: MEMS; Multi-sensor; Wet anisotropic etching; Anodic bonding

1. Introduction

Small unmanned aerial vehicles, which can be applied in more severe environments, have undergone considerable development in the aviation industry [1]. For aerial vehicles, reliable monitoring of the flight parameter to estimate the flight state of the system is crucial to maintaining flight safety in the flight conditions. Information on the flight parameters can be obtained by using all kinds of sensors which are assembled in the flight device. However, due to the limitations of small unmanned aerial vehicles about the size, price and severe application environment, the application of conventional sensors is strongly impeded. However, monolithic multi-sensors can meet the requirements of the small, unmanned aerial vehicle, which characteristically have small volume, low cost and high reliability based on microelectromechanical (MEMS) technology [2, 3]. The monolithic multi-sensor is important for minimizing system size, simplifying the configuration of the system and reducing the cost of the system. These multi-sensors have also been developed in wide range of application fields, extending from environmental monitoring [4, 5] to industrial automation [6, 7] and chemical analysis [8], etc. Among them, some multi-sensors had applied SOI material to improve the environment adaptability of silicon devices, especially for temperature adaptability, because the SiO_2 buried layer under the active silicon in the SOI wafer can provide very good electrical insulation from the silicon substrate to avoid the effect of the leakage current in the piezojunction and reduce the thermal noise of device [9, 10].

In order to meet the requirements of small unmanned aerial vehicles, a monolithic multi-sensor is presented by using the SOI technology, which can simultaneously measure these flight parameters of three-axis acceleration, absolute pressure and tem-

*Corresponding author. Tel.: +86 029 82668616 151
E-mail address: xjb0510@163.com
DOI 10.1007/s12206-008-0105-6

perature in one chip. In the monolithic multi-sensor, the three-axis accelerometer and absolute pressure sensor is based on piezoresistive sensing principles, and the temperature sensor is based on positive temperature response of an ion-implanted thermistor [11]. The multi-sensor chip is fabricated on (100) SOI wafer by using piezoresistive bulk-micromachining technology and silicon-on-glass anodic bonding technology. The piezoresistive bulk-micromachining technology involves ion-implanted piezoresistors and thermistor formation on the front side and the anisotropic etching process [12] on the backside of wafer. The silicon-on-glass anodic bonding technology involves the formation of a vacuum chamber for the absolute pressure sensor and protection structure for the accelerometer. In the paper, the detailed design, fabrication and measurement process of the monolithic multi-sensor is described.

2. The multi-sensor design

Fig. 1 shows the cross-section of the monolithic multi-sensor chip, which consists of a three-axis accelerometer, an absolute pressure sensor and a temperature sensor. The chip size is 4×6×0.9 mm^3.

2.1 Three-axis accelerometer

The accelerometer structure is shown in Fig. 1. The three-axis piezoresistive accelerometer in the chip uses four deflectable cantilever beams which support a silicon seismic mass at its free end. This type of accelerometer has the advantage of high sensitivity; moreover the structure of geometric symmetry can reduce the cross-axis sensitivity. The Pyrex glass substrate bonded by anodic bonding technology provides protection to the movable structure from overloaded acceleration. The narrow air gap between the seismic mass and the Pyrex glass provides the movable space of the seismic mass of the three-axis accelerometer. The finite element method (FEM) simulation software (ANSYS) is used to simulate the stress distribution of the accelerometer structure when the acceleration is loaded. Fig. 2 shows the results of FEM simulation when 1g acceleration for X, Y and Z is applied to the three-axis accelerometer. According to the result of the FEM simulation and the limit of the fabrication technology, the beam length, width and thickness and the seismic mass length, width and thickness are 450μm, 150μm, 35μm, 960μm, 960μm, 395μm, respectively. The layout of piezoresistors is determined by the stress distribution of the four beams. Fig. 3 shows the layout of piezoresistors for the three-axis accelerometer. In order to obtain the maximum sensitivity, the piezoresistors are placed along [110] and [110] crystal orientation which reaches the maximum piezoresistive coefficient of the (100) silicon [13]. The Wheatstone bridge circuits consist of these piezoresistors. These circuits can detect three-axis acceleration and eliminate the cross-axis sensitivities of acceleration. The three Wheatstone bridge circuits which detect X-, Y- and Z-directional accelerations are shown in Fig. 4.

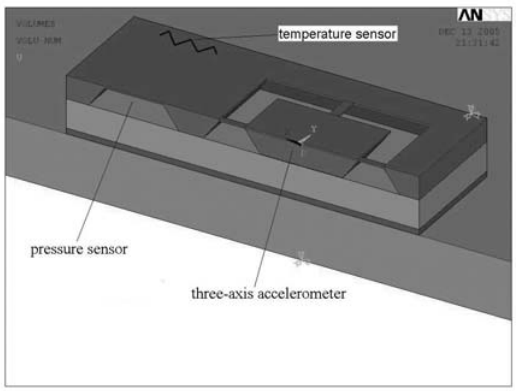

Fig. 1. Cross-section of the monolithic multi-sensor chip.

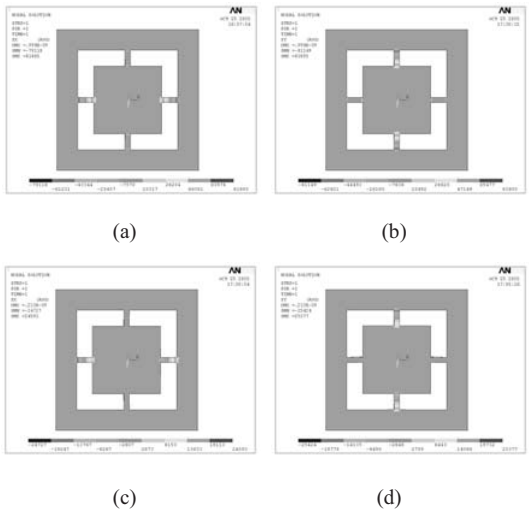

Fig. 2. The stress distribution results of the FEM simulation for acceleration. (a) X directional stress distribution (1g for Z axis); (b) Y directional stress distribution (1g for Z axis); (c) X directional stress distribution (1g for X axis); (d) Y directional stress distribution (1g for Y axis).

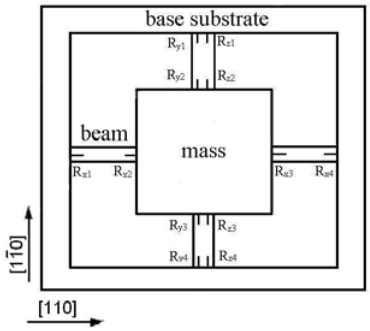

Fig. 3. Arrangement of piezoresistors for three-axis accelerometer.

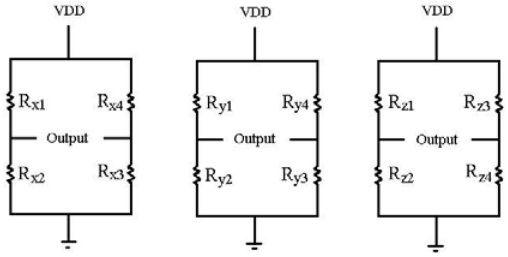

Fig. 4. Three Wheatstone bridge circuits which detect X-, Y- and Z- directional accelerations.

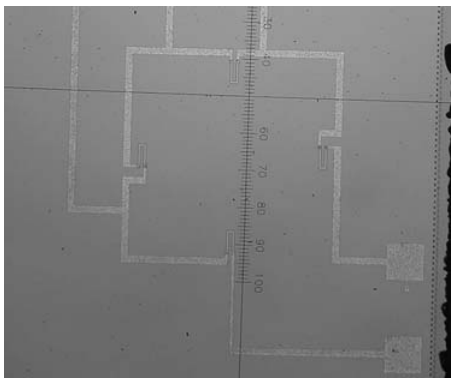

Fig. 5. Photograph of the pressure sensor.

2.2 Pressure sensor

Fig. 5 shows a photograph of the pressure sensor. The thin square diaphragm is fabricated by backside anisotropy wet etching. The diaphragm is the square of 1000μm×1000μm and thickness of 35μm. The vacuum chamber is formed between the diaphragm and the glass substrate by silicon-on-glass anodic bonding technology. The four piezoresistors are placed at the region of the maximal stress on the edge of the diaphragm and form a full Wheatstone bridge

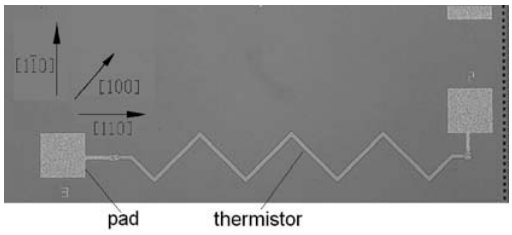

Fig. 6. Photograph of the temperature sensor.

circuit to measure the variety of external pressure. The four piezoresistors are along the crystal orientation of [110]. With a given pressure, the resistance change due to an unbalanced bridge can be directly converted into a voltage signal.

2.3 Temperature sensor

The thermistor of the temperature sensor is fabricated by boron ion-implanted on the active silicon of an SOI wafer. By choosing the appropriate doping concentration, the temperature sensor can provide linear output with change of the environmental temperature. Because the oxide isolation of SOI can eliminate the leakage current of p-n junction isolation between the resistance and silicon substrate, the nonlinear factor of the leakage current can also be avoided. The temperature sensor is placed in the location on the silicon-glass bonding region. In order to minimize the effect of stress on the temperature sensor, the arrangement of the thermistor is along [100] and [010] crystal orientation which reaches the minimum piezoresistive coefficient of the (100) silicon [13]. Fig. 6 shows the structure of the temperature sensor. The temperature sensor is very important for minimizing the effect of temperature in the multi-sensor chip. With the measurement result of the temperature sensor, the external microprocessor can perform suitable digital compensation of temperature to improve multi-sensor accuracy in the monolithic multi-sensor.

3. Device fabrication

The monolithic multi-sensor is fabricated by piezoresistive bulk-micromachining technology and silicon-on-glass anodic bonding technology. The fabrication process of the chip is shown in Fig. 7.

A double-side-polished four-inch N-type (100)-oriented SOI wafer (1.6μm active-silicon, 0.3μm SiO_2 and about 400μm silicon substrate) is used as the

starting material.

The active-silicon is implanted with boron ion. The different implantation dose is, respectively, performed to optimize for piezoresistivity of the piezoresistor and thermal sensitivity of the thermistor in the same wafer. The boron ion implantation dose of piezoresistors is $3.0\times10^{14}cm^{-2}$ and 80kev; the implanted dose of thermistor is $1.5\times10^{16}cm^{-2}$ and 80kev. The ion-implanted active-silicon is annealed in N_2 ambient at 1100℃ for 60 min. The contact area (P+) of piezoresistors is implanted by boron ion with $1.5\times10^{16}cm^{-2}$ to lower the value of the sheet resistance. Finally, the active-silicon is etched by reactive ion etching (RIE) to form the isolated island of piezoresistors and thermistor, which is suitable for applying in a wide temperature range.

In order to fabricate the backside shape of the multi-sensor, including the membrane of accelerometer and pressure sensor, the movable seismic mass and the narrow air gap between the Pyrex glass and the seismic mass, the two-step wet anisotropic etching process on the backside of wafer are applied by using two layer masks in KOH solution. Two photolithographic masks for process of the backside of wafer are shown in Fig. 8. First, two layers of SiO_2/Si_3N_4 (2500Å/1100Å) bi-material film are deposited by LPCVD (see Fig. 7(4)), which is used as two layer masks of wet anisotropic etching on the backside of wafer and protects the piezoresistors and thermistor on the front-side of wafer against the corrosion in the KOH etching solution. The bi-material film of SiO_2/Si_3N_4 can reduce the effect of the thin film stress in the process of film fabrication. Subsequently, two layers of SiO_2/Si_3N_4 bi-material film are patterned according to the shape of two photolithographic masks by RIE and BHF etching as two layer masks of KOH wet etching (see Fig. 7(5)). On the backside of the wafer, the region of the seismic mass is covered by a layer mask of SiO_2/Si_3N_4 bi-material film, the frame region of accelerometer and pressure sensor is covered by two layer masks of bi-material film, and the etching windows are opened in other region. Finally, the anisotropic etching process is performed in two steps (see Fig. 7 (6) and (7)). By the first step, the backside of the accelerometer and pressure sensor is etched in 35% KOH solution at 76℃, and the depth of wet etching is approximately 365μm. A layer mask of SiO_2/Si_3N_4 bi-material film is removed by RIE and BHF etching. In the second step, the backside of the silicon wafer is immersed in KOH solution again to form a narrow air gap (5μm) between the seismic mass and bonded Pyrex glass for movement of the seismic mass and complete the final formation of the backside of accelerometer and pressure sensor. The mask-compensation patterns are performed to the convex corners of the square seismic mass to avoid undercutting of convex corners in the two-step anisotropic etching process. The mask-compensation pattern, in which eight small square masks are arranged at four corners of the square mass mask, is illustrated in Fig. 8(a). The dimension of the small square mask is the depth of wet etching/0.58. A photograph of the anisotropic etching compensation results of square seismic mass is shown in Fig. 9. As shown in the figure, the convex corners of the seismic mass still remain the vertical edge after the wet etching process.

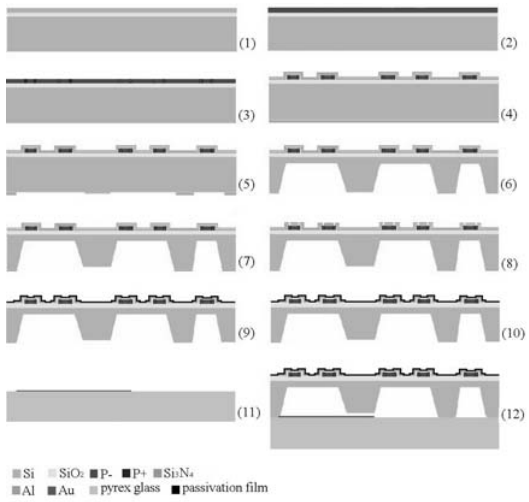

Fig. 7. Fabrication process of the monolithic multi-sensor. (1) SOI wafer. (2) Boron ion-implanted for piezoresistors and thermistor. (3) Boron ion-implanted in the contact area. (4) The island of piezoresistors and thermistor is formed and two layers of SiO_2 and Si_3N_4 bi-material film are deposited. (5) Two layer masks of KOH wet etching are patterned. (6) The first wet anisotropic etching by KOH solution and a layer mask is removed by RIE and BHF etching. (7) The second wet anisotropic etching. (8) The contact holes are etched. (9) The metal wire is formed and the passivation layer is deposited. (10) The suspension beams of accelerometer are fabricated. (11) The metal electrode is sputtered on the Pyrex glass wafer. (12) Anodic bonding between the silicon and Pyrex glass.

The contact holes between the metal wire and the contact area of the piezoresistors, thermistor are formed by RIE on the front side of the wafer. The Ti/Al (1000Å/15000Å) bi-material film deposited by PVD is patterned by dry etching to form the metal

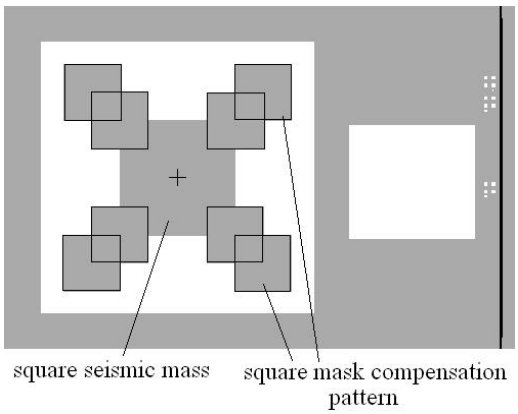

(a)

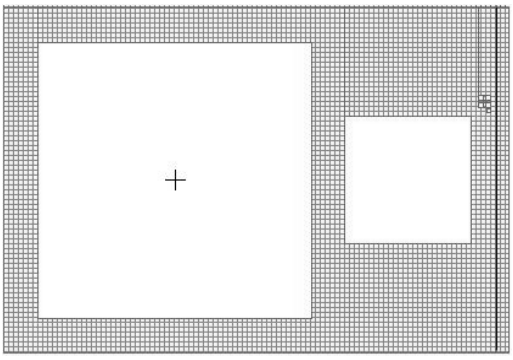

(b)

Fig. 8. Two photolithographic masks for process of the backside of wafer.

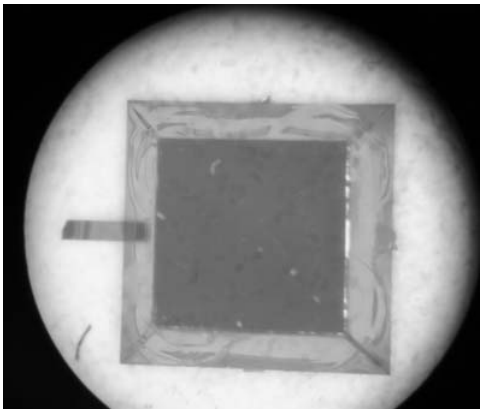

Fig. 9. A photograph of the anisotropic etching compensation results of square seismic mass from the backside of the seismic mass.

wire, then metallization pattern of the metal wire at 480℃. The SiO_2/Si_3N_4 (1000Å/450Å) bi-material film is deposited by PECVD as the passivation layer

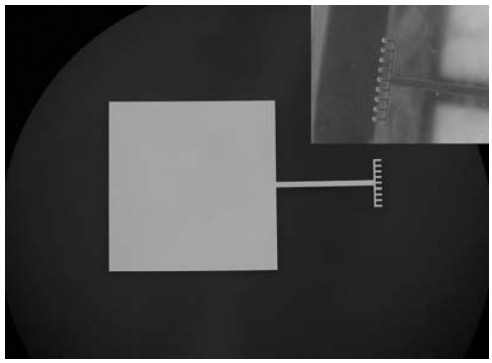

Fig. 10. The structure of the Cr/Au metal electrode on the Pyrex glass and the metal comb by partly inserted into the silicon-glass bonding region.

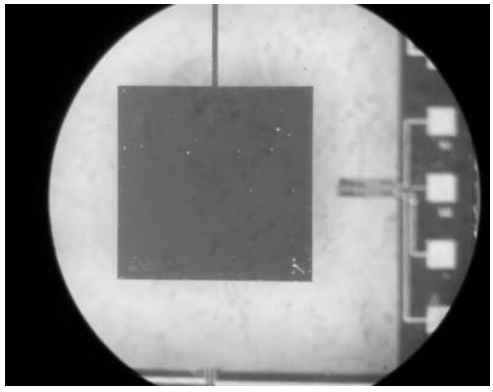

Fig. 11. Photograph of the surface of the metal electrode from the front side of the multi-sensor.

of the device. In the end, the four suspension beams of the accelerometer are fabricated by RIE from the front side of the chip.

The fabricated silicon wafer and Pyrex glass are bonded with anodic bonding technology for encapsulating the accelerometer and forming the vacuum chamber of the pressure sensor. The condition of anodic bonding between silicon and Pyrex glass depends on loading 1000V direct current (DC) voltage and high temperature of 350℃. In the process of anodic bonding, the electrostatic force induced by the strong electric field in the narrow air gap will probably cause the movable silicon seismic mass of accelerometer to stick to the Pyrex glass, resulting in the invalidation of the chip [14]. In order to solve the problem, a Cr/Au (500Å/2000Å) bi-material metal electrode is fabricated. In the Cr/Au bi-material metal electrode, the Cr film provides more adhering force on the cleaning surface of the Pyrex glass. The metal

electrode consists of the metal comb part (comb dent weight: 30μm; length: 100μm) and the flat-plate part (1500μm×1500μm). Fig. 10 shows the whole structure of Cr/Au metal electrode and the metal comb part. The metal electrode is sputtered on the Pyrex glass wafer. The position of the flat-plate part is under the seismic mass of accelerometer, and the metal comb part is arranged to be inserted in the comb dent segment about 10~20μm length into the silicon-glass bonding region for the contact of silicon and the metal electrode. During the anodic bonding process, the flat-plate electrode can keep similar electric potential with the bottom of the seismic mass by the Au-Si contact to prevent the sticking between the seismic mass and Pyrex glass [15]. After the anodic bonding, a surface photograph of the metal electrode is observed in the Fig. 11. From the photograph, no sticking impression is observed on the surface of the metal electrode.

The fabrication process of the monolithic multi-sensor is well suited for batch processing. The multi-sensors are diced and packaged for device evaluation. The monolithic multi-sensor is packaged by the double inline package (DIP). Fig. 12 shows the finished multi-sensor chip and its package.

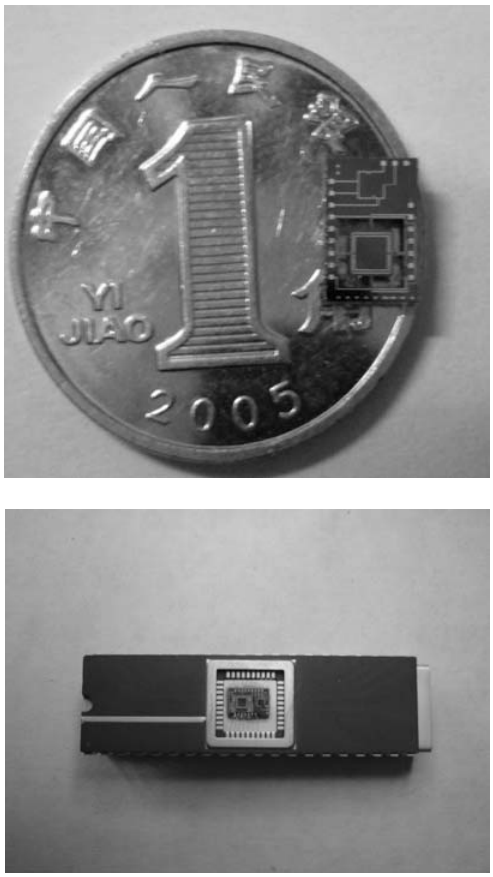

Fig. 12. Photograph of the monolithic multi-sensor and its package.

4. Result

The characteristics of the outputs of the individual sensors in the multi-sensor chip are measured. The three-axis accelerometer of the multi-sensor is measured by using a precision turntable and an ESCORT EDM 3150 precision multimeter, which the 5V DC is supplied to three Wheatstone bridge circuits. Fig. 13 shows the measured output voltages of the three-axis accelerometer for Z, X and Y-axis acceleration at temperature 20℃, respectively. In the range of 0-1g Z-axis acceleration (see Fig. 13(a)), the sensitivity of the Z-axis accelerometer is about 0.102mv $(V \cdot g)^{-1}$, and the cross-axis sensitivity is below 3%. In the range of 0-1g X-axis and Y-axis acceleration (see Fig. 13(b) and (c)), the X-axis and Y-axis sensitivity are about 0.014mv $(V \cdot g)^{-1}$ and 0.014mv $(V \cdot g)^{-1}$, and the maximum cross-axis sensitivity is below 5% in the Z-axis accelerometer. Because the detection principles of the X-axis and Y-axis are equivalent, the output characteristic for Y-axis acceleration is nearly equal with that for X-axis acceleration. In the measured range, non-linearity of the output voltage of Z-axis, X-axis and Y-axis accelerometer is 1.88%FS, 0.83%FS and 1.04%FS, respectively.

The basic output characteristics, temperature and drift characteristics of the absolute pressure sensor are measured by using a precision manometer, a temperature-controlled environmental chamber. Fig. 14 shows the output voltage of the absolute pressure sensor at 20℃ and 70℃, when the 5V DC is supplied. In the range of 0-200KPa, the measured sensitivity of the pressure sensor is 0.020mv $(V \cdot KPa)^{-1}$ at 20℃, and 0.0197mv $(V \cdot KPa)^{-1}$ at 70℃. Non-linearity of the output of the pressure sensor is 0.4%FS at 20℃, and 0.1%FS at 70℃ in the same measured range. The offset of the pressure sensor is 0.467mv at 20℃. Fig. 15 shows the relationship between temperature coefficient of offset (TCO) shift of pressure sensor and the temperature change in the range of 25℃~140℃. Fig. 16 shows the temperature coefficient of sensitivity (TCS) shift in the same temperature range. Its TCO shift is obtained from -3.45×10^{-5}℃$^{-1}$ to -1.70×10^{-4}℃$^{-1}$

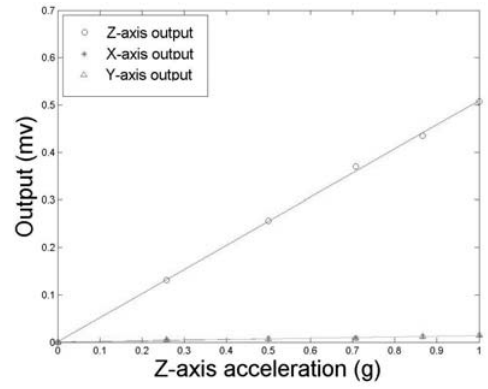

(a)

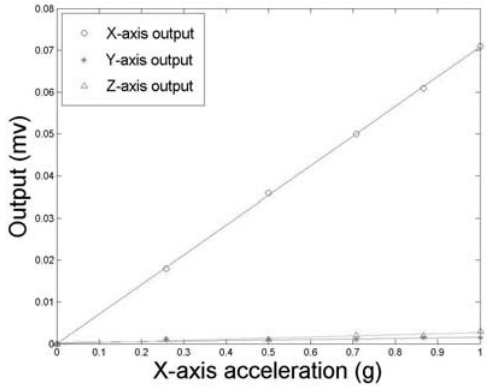

(b)

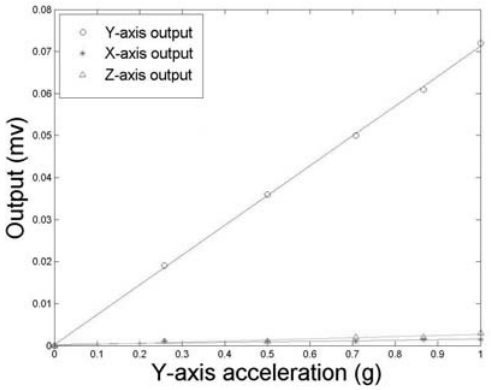

(c)

Fig. 13. Output of the three-axis accelerometer. (a) For Z-axis acceleration input; (b) For X-axis acceleration input; (c) For Y-axis acceleration input.

and the TCS shift is from -2.11×10^{-5}℃$^{-1}$ to -1.93×10^{-3}℃$^{-1}$ in the temperature range. The measured TCO and TCS result of the pressure sensor means that the pressure sensor has the ability to be used in the temperature environment in the range of 20℃~140℃. Because the piezoresistors of the three-axis accelerometer on the multi-sensor are the same boron ion doped dose as that of the pressure sensor, the accelerometer has similar temperature adaptability in the temperature range, too. When the Z-axis acceleration is applied to the three-axis accelerometer in the multi-sensor, due to the lightweight mass of the diaphragm of pressure sensor, the acceleration sensitivity of pressure sensor is below 1.6×10^{-5}mv $(V \cdot g)^{-1}$.

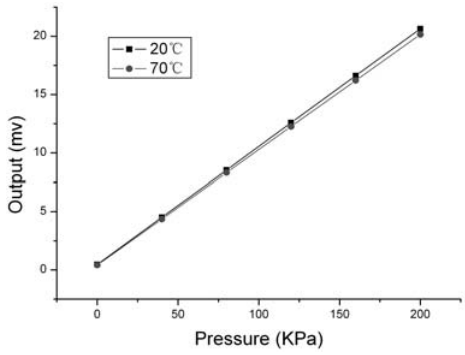

Fig. 14. Output of absolute pressure sensor.

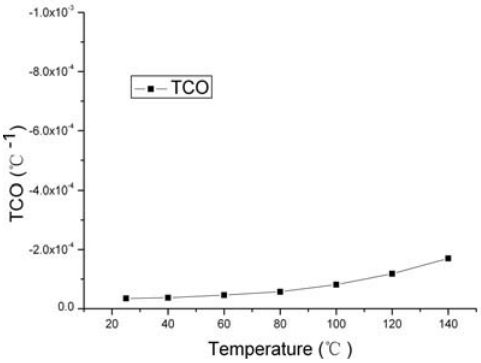

Fig. 15. TCO shift of the pressure sensor as a function of temperature.

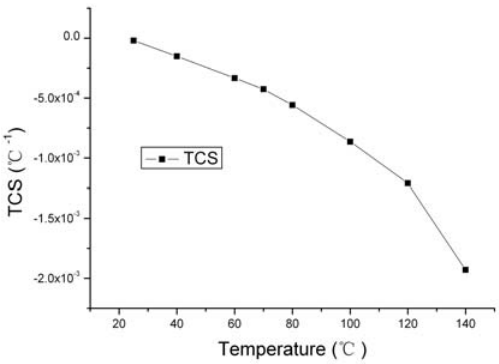

Fig. 16. TCS shift of the pressure sensor as a function of temperature.

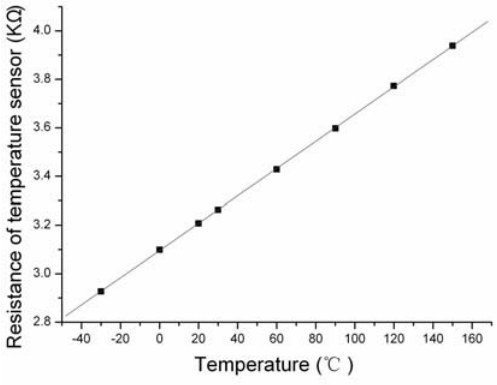

Fig. 17. Output of the temperature sensor.

The thermistor temperature sensor is also measured in a temperature-controlled environmental chamber. The response of the temperature sensor is shown in Fig. 17. The sensitivity of the temperature sensor is 5.617×10^{-3}KΩ · ℃$^{-1}$. The non-linearity of the temperature sensor is 0.48%FS in -30℃~150℃. The temperature coefficient of resistance (TCR) of the temperature sensor is determined to 1.75×10^{-3}℃$^{-1}$. By choosing the appropriate doped dose of Boron ion, the output of the temperature sensor can maintain good linearity in the whole temperature range. Due to the location and the crystal orientation arrangement of the temperature sensor in the multi-sensor, the temperature sensor can avoid the effect of stress, when the external acceleration and pressure is changed in the measure range.

5. Conclusion

A prototype of the monolithic multi-sensor for the small unmanned aerial vehicle, which is capable of monitoring three-axis acceleration, pressure and temperature, is reported by using SOI wafers. The design, fabrication and measurement process of the monolithic multi-sensor are presented in the paper. The measured results show that the multi-sensor has good output characteristics about three-axis acceleration, pressure and temperature in a wide temperature range environment, which means the feasibility of using the multi-sensor in flight device fields. Future work will be required to optimize the response and the fabrication process of the multi-sensor.

References

[1] D. H. Lyon, A military perspective on small unmanned aerial vehicles, *IEEE Instrumentation & Measurement Magazine*. 7 (3) (2004) 27-31.

[2] D. Gebre-Egziabher, R. C. Hayward and J. D. Powell, Design of multi-sensor attitude determination systems, IEEE Trans. Aerospace and Electronic Systems. 40 (2004) 627-649.

[3] A. Mason, N. Yazdi, A. V. Chavan, K. Najafi and K. D. Wise, A generic multielement microsystem for portable wireless applications, Proceedings of the IEEE. 86 (1998) 1733-1746.

[4] T. Fujita and K. Maenaka, Integrated multi-environmental sensing-system for the intelligent data carrier, Sens. Actuat. A. 97-98 (2002) 527-534.

[5] A. Hyldgard, O. Hansen and E. V. Thomsen, Fish & chips: single chip silicon MEMS CTDL salinity, temperature, pressure and light sensor for use in fisheries research, Proc. 18th IEEE Int.Conf. on Micro Electro Mechanical Systems, Miami Beach, Florida, USA. (2005) 303-306.

[6] A. D. DeHennis and K. D. Wise, A wireless microsystem for the remote sensing of pressure, temperature, and relative humidity, *J. Microelectromech. Syst*. 14 (2005) 12-22.

[7] K. I. Lee, H. Takao, K. Sawada and M. Ishida, Low temperature dependence three-axis accelerometer for high temperature environments with temperature control of SOI piezoresistors, Sens. Actuat. A. 104 (2003) 53-60.

[8] P. Norlin, O. Ohman, B. Ekstrom and L. Forssen, A chemical micro analysis system for the measurement of pressure, flow rate, temperature, conductivity, UV-absorption and fluorescence, Sens. Actuat. B. 49 (1997) 34-39.

[9] T. Nakamura, SOI technologies for sensor, Proc. 7th Int. Conf. on Solid-State Sensors and Actuators (Transducers '93), Yokohama, Japan. (1993) 230-232.

[10] B. Diem, P. Rey, S. Renard, S. Viollet Bosson, H. Bono, F. Michel, M. T. Delaye and G. Delapierre, SOI SIMOX; from bulk to surface micromachining, a new age for silicon sensors and actuators, Sens. Actuat. A. 46-47 (1995) 8-16.

[11] N. D. Arora, J. R. Hauser and D. J. Roulston, Electron and hole mobilities in silicon as a function of concentration and temperature, IEEE Trans. Electron Devices. 29 (1982) 292-295.

[12] J. Fruhauf and B. Hannemann, Anistropic multistep etch processes of silicon, *J. Micromech. Microeng*. 7 (1997) 137-140.

[13] Y. Kanda, A graphical representation of the pie-

zoresistance coefficients in silicon, IEEE Trans. Electron Devices. 29 (1982) 64-70.

[14] N. Ito, K. Yamada, H. Okada, M. Nishimura and T. Kuriyama, A rapid and selective anodic bonding method, Proc. 8th Int. Conf. on Solid-state Sensors and Actuators, and Eurosensors IX (Transducers '95), Stockholm, Sweden. (1995) 277-280.

[15] Z. H. Li, Y. L. Hao, D. C. Zhang, T. Li and G. Y. Wu, An SOI-MEMS technology using substrate layer and bonded glass as wafer-level package, Sens. Actuat. A. 96 (2002) 34-42.